Available on CMS information server

CMS CR -2016/033

The Compact Muon Solenoid Experiment

Conference Report

Mailing address: CMS CERN, CH-1211 GENEVA 23, Switzerland

08 March 2016

R and D on a new type of micropattern gaseous detector the Fast Timing Micropattern detector.

Ilaria Vai for the CMS Collaboration

Abstract

Micropattern gaseous detectors (MPGD) underwent significant upgrades in recent years, introducing resistive materials to build compact spark-protected devices. Exploiting this technology further, various features such as space and time resolution, rate capability, sensitive area, operational stability and radiation hardness can be improved. This contribution introduces a new type of MPGD, namely the Fast Timing Micropattern (FTM) detector, utilizing a fully resistive WELL structure. It consists of a stack of several coupled layers where drift and WELL multiplication stages alternate in the structure, yielding a significant improvement in timing properties due to competing ionization processes in the different drift regions. Two FTM prototypes have been developed so far. The first one is uWELL-like, where multiplication takes place in the holes of a kapton foil covered on both sides with resistive material. The second one has a resistive Micromegas-like structure, with multiplication developing in a region delimited by a resistive mesh. The structure of these prototypes will be described in detail and the results of the characterization study performed with an X-Ray generator with two different gas mixtures will be presented. First results on rate capability and time resolution based on data collected with cosmic rays and muon/pion test beams will also be presented.

Presented at *VCI 2016 14th Vienna Conference on Instrumentation*

R&D on a new type of micropattern gaseous detector: the Fast Timing Micropattern detector

D. Abbaneo[r], M. Abbas[r], M. Abbrescia[b], A.A. Abdelalim[i], M. Abi Akl[n], O. Aboamer[h], D. Acosta[p], A. Ahmad[t], W. Ahmed[i], W. Ahmed[t], A. Aleksandrov[ac], R. Aly[i], P. Altieri[b], C. Asawatangtrakuldee[c], P. Aspell[r], Y. Assran[h], I. Awan[t], S. Bally[r], Y. Ban[c], S. Banerjee[u], V. Barashko[p], P. Barria[e], G. Bencze[g], N. Beni[k], L. Benussi[o], V. Bhopatkar[x], S. Bianco[o], J. Bos[r], O. Bouhali[n], A. Braghieri[aa], S. Braibant[d], S. Buontempo[z], C. Calabria[b], M. Caponero[o], C. Caputo[b], F. Cassese[z], A. Castaneda[n], S. Cauwenbergh[s], F.R. Cavallo[d], A. Celik[j], M. Choi[ag], S. Choi[ae], J. Christiansen[r], A. Cimmino[s], S. Colafranceschi[r], A. Colaleo[b], A. Conde Garcia[r], S. Czellar[k], M.M. Dabrowski[r], G. De Lentdecker[e], R. De Oliveira[r], G. de Robertis[b], S. Dildick[j,s], B. Dorney[r], W. Elmetenawee[i], G. Endroczi[g], F. Errico[b], A. Fenyvesi[k], S. Ferry[r], I. Furic[p], P. Giacomelli[d], J. Gilmore[j], V. Golovtsov[q], L. Guiducci[d], F. Guilloux[ab], A. Gutierrez[m], R.M. Hadjiiska[ac], A. Hassan[i], J. Hauser[w], K. Hoepfner[a], M. Hohlmann[x], H. Hoorani[t], P. Iaydjiev[ac], Y.G. Jeng[ag], T. Kamon[j], P. Karchin[m], A. Korytov[p], S. Krutelyov[j], A. Kumar[l], H. Kim[ag], J. Lee[ag], T. Lenzi[e], L. Litov[ad], F. Loddo[b], A. Madorsky[p], T. Maerschalk[e], M. Maggi[b], A. Magnani[aa], P.K. Mal[f], K. Mandal[f], A. Marchioro[r], A. Marinov[r], R. Masod[h], N. Majumdar[u], J.A. Merlin[r,ah], G. Mitselmakher[p], A.K. Mohanty[y], S. Mohamed[h], A. Mohapatra[x], J. Molnar[k], S. Muhammad[t], S. Mukhopadhyay[u], M. Naimuddin[l], S. Nuzzo[b], E. Oliveri[r], L.M. Pant[y], P. Paolucci[z], I. Park[ag], G. Passeggio[z], B. Pavlov[ad], B. Philipps[a], D. Piccolo[o], H. Postema[r], A. Puig Baranac[r], A. Radi[h], R. Radogna[b], G. Raffone[o], A. Ranieri[b], G. Rashevski[ac], C. Riccardi[aa], M. Rodozov[ac], A. Rodrigues[r], L. Ropelewski[r], S. RoyChowdhury[u], G. Ryu[ag], M.S. Ryu[ag], A. Safonov[j], S. Salva[s], G. Saviano[o], A. Sharma[b], A. Sharma[r], R. Sharma[l], A.H. Shah[l], M. Shopova[ac], J. Sturdy[m], G. Sultanov[ac], S.K. Swain[f], Z. Szillasi[k], J. Talvitie[v], A. Tatarinov[j], T. Tuuva[v], M. Tytgat[s], I. Vai[aa,*], M. Van Stenis[r], R. Venditti[b], E. Verhagen[e], P. Verwilligen[b], P. Vitulo[aa], S. Volkov[q], A. Vorobyev[q], D. Wang[c], M. Wang[c], U. Yang[af], Y. Yang[e], R. Yonamine[e], N. Zaganidis[s], F. Zenoni[e], A. Zhang[x]

[a] *RWTH Aachen University, III Physikalisches Institut A, Aachen, Germany*
[b] *INFN Bari and University of Bari, Bari, Italy*
[c] *Peking University, Beijing, China*
[d] *INFN Bologna and University of Bologna, Bologna, Italy*
[e] *Universite Libre de Bruxelles, Brussels, Belgium*
[f] *National Institute of Science Education and Research, Bhubaneswar*
[g] *Institute for Particle and Nuclear Physics, Wigner Research Centre for Physics, Hungarian Academy of Sciences, Budapest, Hungary*
[h] *Academy of Scientific Research and Technology - Egyptian Network of High Energy Physics, ASRT-ENHEP, Cairo, Egypt*
[i] *Helwan University & CTP, Cairo, Egypt*
[j] *Texas A&M University, College Station, U.S.A.*
[k] *Institute for Nuclear Research of the Hungarian Academy of Sciences (ATOMKI), Debrecen, Hungary*
[l] *University of Delhi, Delhi, India*
[m] *Wayne State University, Detroit, U.S.A*
[n] *Texas A&M University at Qatar, Doha, Qatar*
[o] *Laboratori Nazionali di Frascati - INFN, Frascati, Italy*
[p] *University of Florida, Gainesville, U.S.A.*
[q] *Petersburg Nuclear Physics Institute, Gatchina, Russia*
[r] *CERN, Geneva, Switzerland*
[s] *Ghent University, Dept. of Physics and Astronomy, Ghent, Belgium*
[t] *National Center for Physics, Quaid-i-Azam University Campus, Islamabad, Pakistan*
[u] *Saha Institute of Nuclear Physics, Kolkata, India*
[v] *Lappeenranta University of Technology, Lappeenranta, Finland*
[w] *University of California, Los Angeles, U.S.A.*
[x] *Florida Institute of Technology, Melbourne, U.S.A.*
[y] *Bhabha Atomic Research Centre, Mumbai, India*
[z] *INFN Napoli, Napoli, Italy*
[aa] *INFN Pavia and University of Pavia, Pavia, Italy*
[ab] *IRFU CEA-Saclay, Saclay, France*
[ac] *Institute for Nuclear Research and Nuclear Energy, Sofia, Bulgaria*
[ad] *Sofia University, Sofia, Bulgaria*
[ae] *Korea University, Seoul, Korea*
[af] *Seoul National University, Seoul, Korea*
[ag] *University of Seoul, Seoul, Korea*
[ah] *Institut Pluridisciplinaire - Hubert Curien (IPHC), Strasbourg, France*

Abstract

This contribution introduces a new type of Micropattern Gaseous Detector, the Fast Timing Micropattern (FTM) detector, utilizing fully Resistive WELL structures. The structure of the prototype will be described in detail and the results of the characterization study performed with an X-ray gun will be presented, together with the first results on time resolution based on data collected with muon/pion test beams.

Keywords: Micropattern Gaseous Detectors, RWELL, Time resolution, CMS
PACS: 29.40.Cs, 29.40.Gx

Preprint submitted to Elsevier *March 7, 2016*

1. Introduction

Time resolution of classical Micropattern Gas Detectors (MPGD), like Gas Electron Multiplier (GEM) and Micromegas, is dominated by the fluctuations on the position on the first ionization cluster in the drift gap. The average time needed for the nearest ionization cluster to reach the amplification stage is indeed given by $t = d / v_d$, where d is the distance of the closest cluster to the first amplification region and follows the distribution $e^{-\lambda x}/\lambda$, where λ is the average number of primary clusters generated by an ionising particle inside the gas per unit lenght; v_d instead is the drift velocity, that depends on the gas mixture and the applied drift field. The contribution to the time resolution of the drift velocity is $\sigma_t = (\lambda v_d)^{-1}$: with a typical drift gap of the order of 3-4 mm and with a proper choice of the gas mixture, MPGDs can reach a time resolution of the order of 5-10 ns. An improvement in the time resolution, to reach the 1 ns scale, can be obtained working on the segmentation of the drift gap: the principle is to divide a single thick drift region in many thinner drift regions, each coupled to its amplification stage. The reduction in time resolution that can be obtained is so proportional to the number of stages N_D employed: $\sigma_t = (\lambda v_d N_D)^{-1}$. The first prototype of Fast Timing Micropattern (FTM) detector exploits this principle using two 250 μm-thick drift gaps, each coupled with an amplification region composed by a fully resistive WELL. The construction of consecutive drift-amplification stages is allowed by the use of resistive layers to polarize drift and multiplication volumes. The overall structure is then transparent to the signal that can be extracted from every amplification stage.

2. The Fast Timing Micropattern detector

The structure of the first prototype of Fast Timing Micropattern (FTM) detector is described in [1]. It is composed by two

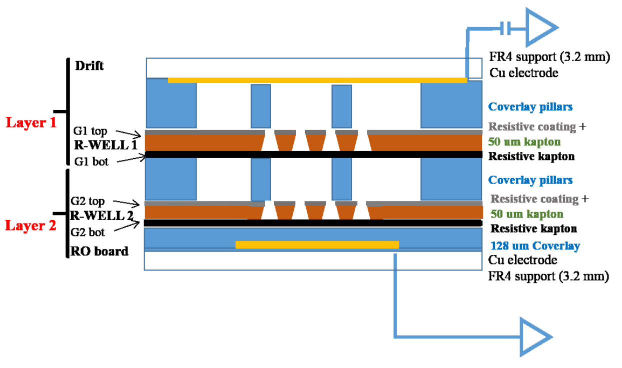

Figure 1: Transversal view of the first prototype of FTM detector.

independent drift-amplification stages (Fig.1): each amplification region is based on a pair of polyimide foils, i.e. kapton, stacked due to the electrostatic force induced by the polarization of the foils: the first foil, perforated with inverted truncated-cone-shaped holes (with top base 100 μm and bottom base 70 μm and pitch 140 μm), is a 50 μm thick polyimide foil (Apical) from KANECA, coated with diamond-like carbon (DLC) technique, to reach up to 800 MΩ/□; the second foil is 25 μm thick XC Dupont Kapton, with a resistivity of 2 MΩ/□. The drift volumes are 250 μm thick, with planarity ensured by coverlay pillars, 400 μm diameter and pitch of 3.3 mm. The active area of the prototype is of the order of 20 cm^2. The induced signal can be picked up from the readout electrode, but also from the drift electrode, through a capacitive coupling.

3. Characterization with X-Ray

The first characterization of the FTM prototype was performed at CERN with a Amptek Mini-X X-ray tube, with Ag cathode filament (22 keV X-Rays). Examples of signals picked up from the drift and readout electrodes and read out with an electronics chain composed by a preamplifier ORTEC 142PC and an amplifier ORTEC 474, are shown in Fig.2.

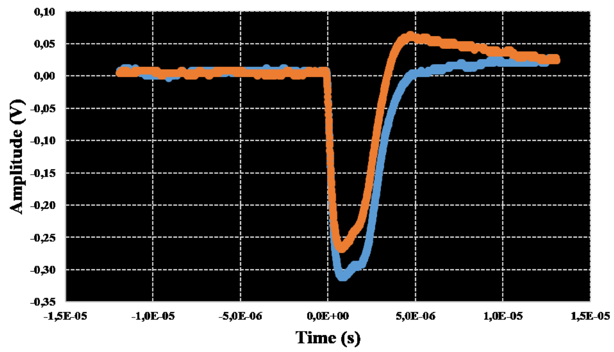

Figure 2: Signals from the FTM detector after amplification and shaping made with a preamplifier ORTEC 142PC and an amplifier ORTEC 474: in blue the signal pickup from the readout electrode, in orange from the drift electrode through a capacitive coupling, the latter being inverted.

The rate from both the readout and drift electrodes at different values of current from the X-Ray gun, i.e different values of incident flux up to the maximum available from the source, is shown in Fig.3. The response of the detector, for both the electrodes, is linear; in addition the two data sets are comparable, giving an indication of the electrical transparency of the layers.

4. Time resolution measurement

A two-week test beam was carried out in autumn 2015 at the SPS H4 beam line [2] at CERN, with muon and pion beams, with the aim of measuring the time resolution of the detector. The setup used during the test and shown in Fig.4 was instrumented with three 10 × 10 cm^2 Triple-GEM detectors, 3:2:2:2 mm gap configuration, for alignment with the beam and four scintillators, including one 2.5 × 3.5 cm^2 finger scintillator, for triggering.

The time resolution was evaluated with muon and pion beams in different powering configuration of the detector.

*Corresponding author
Email address: ilaria.vai@cern.ch (I. Vai)

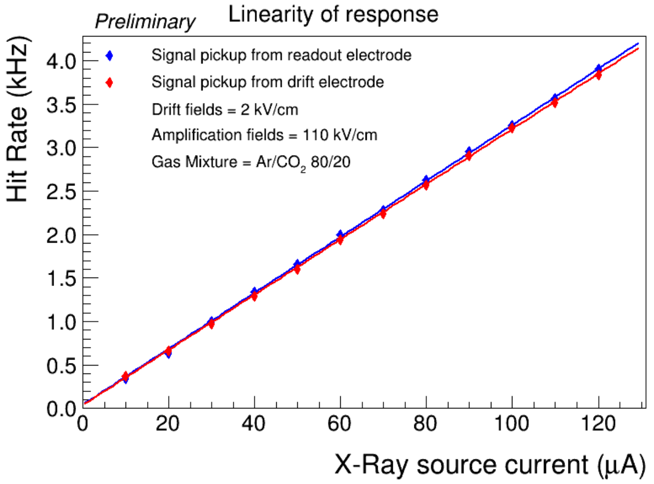

Figure 3: Measured hit rate from both channels of the FTM detector as a function of the X-ray current, which is proportional to the incident flux, up to the maximum available from the source. The increase of the rate measured is linear with the increase of the incident flux. In addition, the data sets from readout and drift channels are comparable, outlining the electrical transparency of the layers.

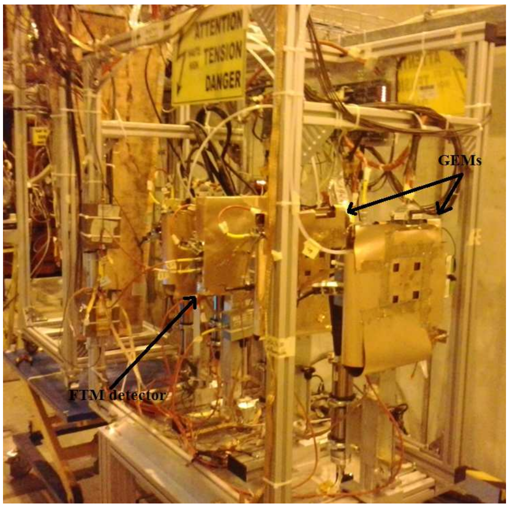

Figure 4: Stand used for the time resolution measurement during 2015 test beam: from the front, two 10×10 cm^2 Triple-GEM, the FTM detector with the squared copper case and the last Triple-GEM for alignment. The four scintillators are placed behind each detector, in particular the finger scintillator is placed just behind the FTM detector in order to match the active area of the prototype and improve the geometrical acceptance of the trigger.

Fig.5 shows the time distribution of events induced by muons: the signal is taken from the drift electrode and read out by a fast electronic chain composed by a Cividec broadband amplifier and a linear Lecroy 612AM amplifier. The time resolution is the sigma of the gaussian fit to the time distribution and is of the order of 2.5 ns. The same result obtained with pions is shown in Fig.6: here the time resolution is of the order of 1.7 ns. All these results were achieved using a green-house-gas-free gas mixture, composed by Ar/CO_2 70/30.

Fig.7 shows instead the measured time resolution for different values of applied drift fields, keeping constant the amplification fields, with both muon and pion beams. The time resolution of the detector seems not to be affected by a change in drift field: this is due to the fact that, with such a small drift gap, even a big change in the drift velocity would not affect significantly the time needed by electrons to reach the amplification region. In addition, the drift velocity in Ar/CO_2 70/30 mixture can be considered almost constant, with variations of the order of 5% for drift fields between 2 and 10 kV/cm [3].

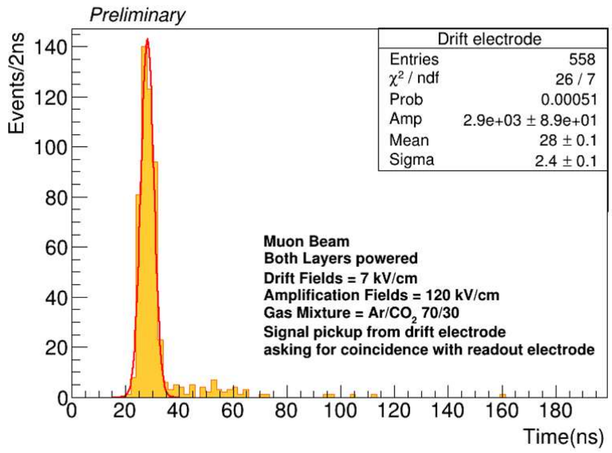

Figure 5: Detector time distribution of the events induced by muons during 2015 test beam. The time resolution was evaluated from the sigma of the gaussian fit.

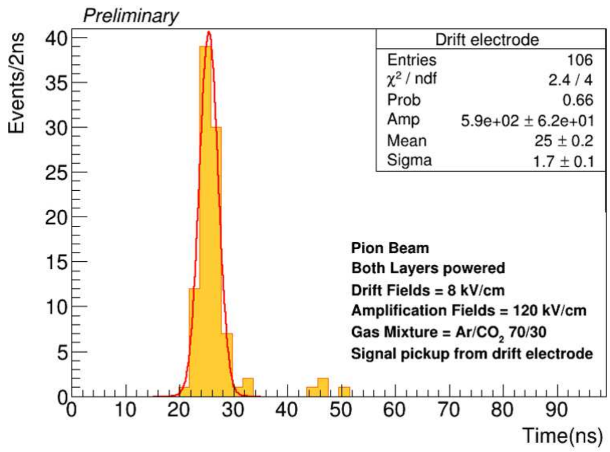

Figure 6: Detector time distribution of the events induced by pions during 2015 test beam. The time resolution was evaluated from the sigma of the gaussian fit.

Recalling the formula $\sigma_t = (\lambda v_d N_D)^{-1}$ we can make a rough estimation of the time resolution expected for a two layers detector: assuming $\lambda \sim 33cm^{-1}$ for MIP in Ar/CO_2 70/30 mixture, $v_d \sim 8$ cm/μs, the estimated time resolution is $\sigma_t \sim 1.9$ ns, in good agreement with the results obtained.

5. Application in High Energy Physics experiments: the CMS muon system in the high η region

With the improvement in luminosity foreseen for High-Luminosity LHC, also the flux of particles through the CMS detector will greatly exceed that in previous running. Keeping

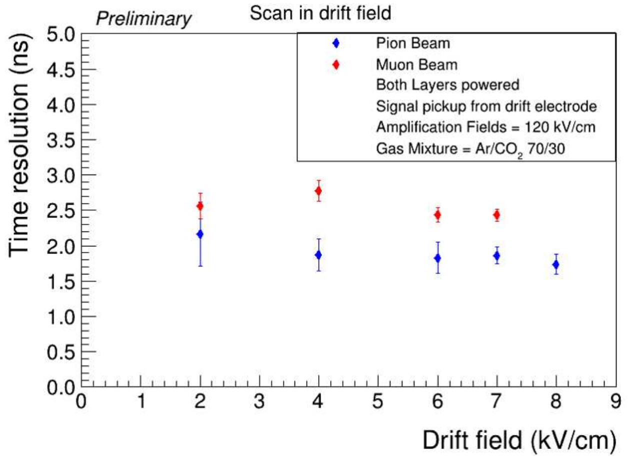

Figure 7: Measured time resolution for different values of applied drift field: the red points refer to muon beam, the blue ones to pion beam.

the same performance of Run 1 will be a great challenge for the collaboration. In particular, focusing on the high pseudorapidity (η) region of the muon system of the CMS experiment the biggest challenges will be:

- Redundancy: the high η region is the region with the highest rates but the fewest muon layers;
- Rate: increases towards higher η;
- Detector Longevity: after years of LHC operation the accumulated charge will reach values of the order of few C/cm^2;
- Electronics: the existing electronics is not able to handle the occupancies/rates and latencies.

In order to face this conditions the CMS Collaboration decided to improve the muon system, also with the introduction of new stations instrumented with MPGDs, as shown in Fig.8. The GEM Endcap 1/1 (GE1/1) station will be instrumented with GEM detectors and installed during Long Shutdown 2 (LS2) [4]; for the other two stations proposed for LS3, GE2/1 and ME0 (Muon Endcap 0), the baseline solution is again GEM detectors, but optional solutions foresee μRWELL technology [5] for GE2/1 and the FTM technology for ME0.

The purpose of the ME0 station in particular is the increase in pseudorapidity coverage and acceptance up to $|\eta| < 3$. In addition, in order to match with the new tracker that will provide triggering up to $|\eta| < 2.4$, the ME0 station should also provide a robust muon trigger with low p_T threshold and muon tagging. The conditions in which the station would have to operate will be extremely harsh, with a pile-up of the order of 140-200 and a very high background rate up to 100 kHz/cm^2. For these reasons the detectors to be installed in the proposed station will need to have:

- High granularity and spatial segmentation, to allow p_T assignement and improve pile-up rejection;

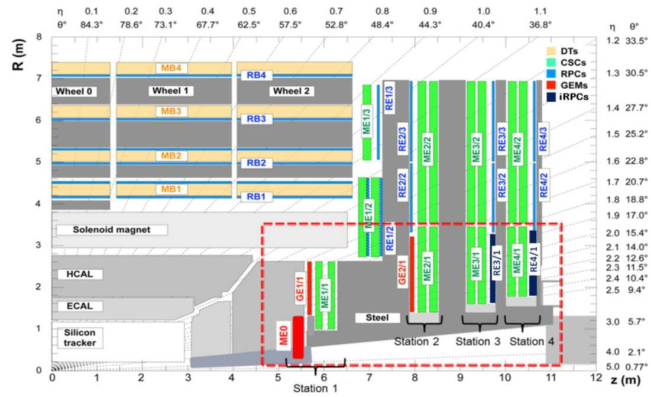

Figure 8: The CMS muon system instrumented with MPGD.

- Multi-layered structure, to allow an improvement of local muon track recontruction and discrimination between muons (resulting in a segment) and neutrons (resulting in uncorrelated hits);
- Timing, to allow object reconstruction, reduction of in-time pile up and help in vertex association. Also neutron background mitigation will benefit from timing: if the detection location is known precisely, only small time windows are compatible with genuine muon hits from the interaction point.

6. Summary

The first prototype of Fast Timing Micropattern detector was tested and proved to have a linear response to the rate, to be electrically transparent and its time resolution was measured to be of the order of 1.5-2.5 ns with Ar/CO_2 70/30 gas mixture.

The detector is being considered for applications in high energy physics experiments, like CMS muon system.

The R&D is ongoing with the design of a new prototype, fully PCB-based, with at least 4 independent stages, that will be tested at the SPS facility and at the Gamma Irradiation Facility (GIF++) [6] at CERN in presence of high gamma-ray background.

Acknowledgments

We gratefully aknowledge the support of FRS-FNRS (Belgium), FWO-Flanders (Belgium), BSF-MES (Bulgaria), BMBF (Germany), DAE (India), DST (India), INFN (Italy), NRF (Korea), QNRF (Qatar), and DOE (USA).

References

[1] R. De Oliveira et al., A novel fast timing micropattern gaseous detector:FTM, arXiv:1503.05330.
[2] SPS infrastucture, http://ab-dep-op-sps.web.cern.ch/ab-dep-op-sps/.
[3] Y. Assran et al., Transport properties of operational gas mixtures used at LHC, arXiv:1110.6761.
[4] CMS GEM Collaboration, CERN-LHCC-2015-012.
[5] G.Becivenni et al., The micro-Resistive WELL detector: a compact spark-protected single amplification-stage MPGD, 2015 JINST 10 P02008.
[6] GIF++, https://espace.cern.ch/sba-workspace/gifpp/SitePages/Home.aspx